IMPROVED PERFORMANCE OF HYBRID ELECTRIC VEHICLES WITH NOVEL REDUCED SWITCH MULTILEVEL QUASI Z INVERTER

Meenakshi THILLAINAYAGAM
Jansons Institute of Technology, Coimbatore, India
meenakshi.t@jit.ac.in

Suthanthiravanitha NARAYANAN
Knowledge Institute of Technology, Salem, India

Abstract: *Hybrid electric vehicles (HEV) have attained a remarkable significance in automotive industry and continuous research is carried on optimisation of HEV. This paper attempts to enhance the performance of HEV by employing new stepped DC link coupled Quasi Z inverter. The proposed inverter aids efficient source management and offers simplified power conditioning circuitry for HEV. The hybrid topology ensures continuous operation of the drive for varied asymmetrical inputs and the self-boost nature lessens the source requirements. The mitigated harmonics with reduced stress on components, poses improved efficiency of 4.87% and reduction in torque ripple by 1% as compared to its predecessor fed to HEV. Simulated and experimental results using the designed prototype validate the proposed theoretical model. Furthermore, this paper analyses all the operating states of the proposed module and the performance of the integrated system is evaluated for various input conditions. Loss calculation and efficiency Assessment is performed to ascertain the advantages of the proposed inverter with HEVs.*
Key words: Fuel cell, Battery, Electric Vehicles, Z source inverter

1. Introduction

Hybrid Electric vehicles have been hailed as an exciting green innovation in transport industry and its credentials include fuel efficiency, environment friendly, quiet in operation and economical. Fuel cells (FCs) have been globally accepted as a primary power source for hybrid electric vehicles and battery is used in HEV to support the drive during power demands [1-2]. Therefore, basically the traction drive system of a HEV consists of a FC stack, a battery pack powered by IC engine, power electronic circuit, and a traction motor [3]. The hybrid input power is used to drive the electric motor associated with the vehicle dynamics and the resources of power electronics are used at various junctures for efficient operation of the HEV [4].

The FCs are sensitive to parametric variations and levies fluctuations in common DC bus voltage. Traditionally, a front-end dc-dc boost converter is scheduled between the energy source and common DC bus to reduce the deviations at the common coupling point. The common DC bus voltage drives the voltage source inverter (VSI) associated to control the traction motor coupled vehicle drive system [5-6]. This two stage conversion increases the complexity and is not an optimal approach always. Hence an alternate was looked for to reduce the task to single stage conversion and Z source inverter (ZSI) was devised [7]. ZSI provides voltage boosting capability by its unique impedance network and shoot through states and eliminates the DC-DC converter stage. Many topologies of ZSI were reported in literature and few to mention are Quasi Z source inverters[8], Improved Z source inverters[9], Extended boost Z source inverters [10-11] and were promoted for HEVs[12-15]. All the aforesaid ZSIs yield two level output voltage rich in harmonics, produces high stress on components and the heavy inrush current during start increases the component rating. Quasi Z network (qZ) for cascaded multilevel inverter was proposed in that yields boosted multilevel output voltage but the use qZ network in each H bridge increases the complexity and decreases the efficiency of the system[16].

This paper on the other hand proposes a modified topology of ZSI, the new stepped DC link quasi Z inverter (SDCqZSI) for HEVs. The configuration uses the hybrid source of fuel cell and battery connected through switching devices to form a stepped DC input eliminating the common coupling and is integrated with the qZSI. The applied stepped circuit uses minimal number of switches compared to other multilevel DC link configurations and adds advantage to the proposed system. The qZSI buck/boost the stepped input voltage and flipping it to yield multilevel AC voltage. The number of levels in the output voltage is decided by the source number at the input.

2. System description

The hybrid electric vehicle (HEV) is composed of hybrid sources and equipped with an electrical traction system to propel the vehicle. The schematic of hybrid electric vehicle with proposed inverter is shown in Fig. 1. The battery is recharged by the DC generator coupled with the internal combustion engine (ICE) and it serves as a secondary source. The voltage output from fuel cell and battery are directly fed as modular units and the single stage conversion of DC to boosted multilevel AC eliminates the intermediate power conditioning stage. The AC output in turn drives the three phase induction motor drive coupled with the continuous variable transmission arrangement [17].

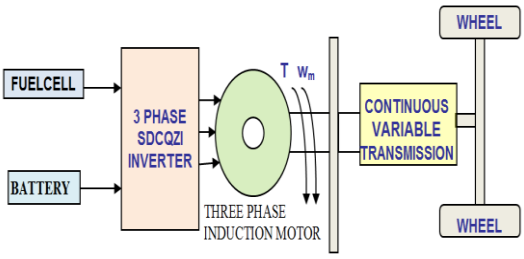

Fig.1. Block Diagram of Hybrid electric vehicle with proposed SDCqZSI.

3. Analysis of proposed stepped dc link fed quasi z inverter

A. Conventional Inverters for HEV

The conventional inverters used in HEVs are shown in Fig. 2. Referring to Fig. 2a, the VSI fed HEV needs a DC-DC converter as an intermediate power conditioning stage to boost the DC bus voltage fed from fuel cell and battery. This decreases the efficiency of the system. On the other hand, the Z source inverter given in Fig. 2b. operates on shoot through states and provides the voltage boosting function desired for fuel cells. The single stage conversion improves the efficiency but the high voltage stress, heavy inrush current and the harmonic content are to be attended to make it more efficient.

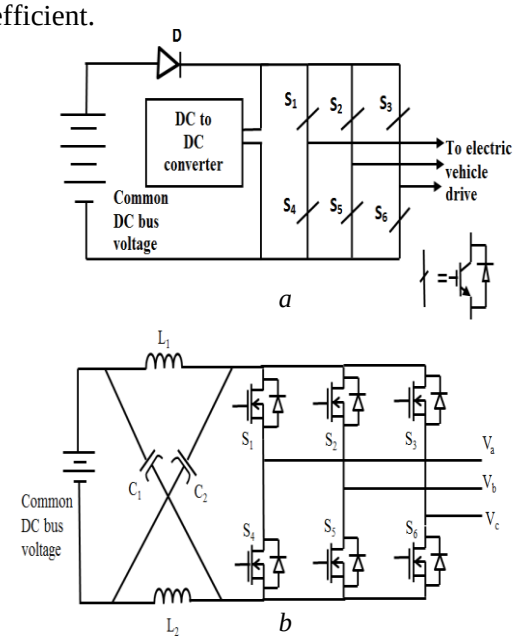

Fig. 2. Structure of conventional inverter fed to Electric Vehicle drive(a) VSI with DC-DC converter(b) Z source inverter

B. Circuit Description of proposed Seven level SDCqZSI

Fig. 3a shows the structure of proposed seven level SDCqZSI. The fuel cell and battery source are combined at specified time interval by the programmed operation of the switching devices to form stepped DC link voltage (V_{sdc}) measured across C_{dc}. The cell source is bypassed with off state, or adds to the dc-link voltage when switch is on. Fundamental switching frequency is implemented on the DC side and the stepped input fed to the QZSI produces boosted multilevel AC voltage. The multilevel reduces the harmonic content in voltage waveform. The multiple switching levels present in the system exposes the components to low switching voltages as compared to conventional Z source inverters and PWM inverters thus reducing dv/dt and voltage stress problems [28].

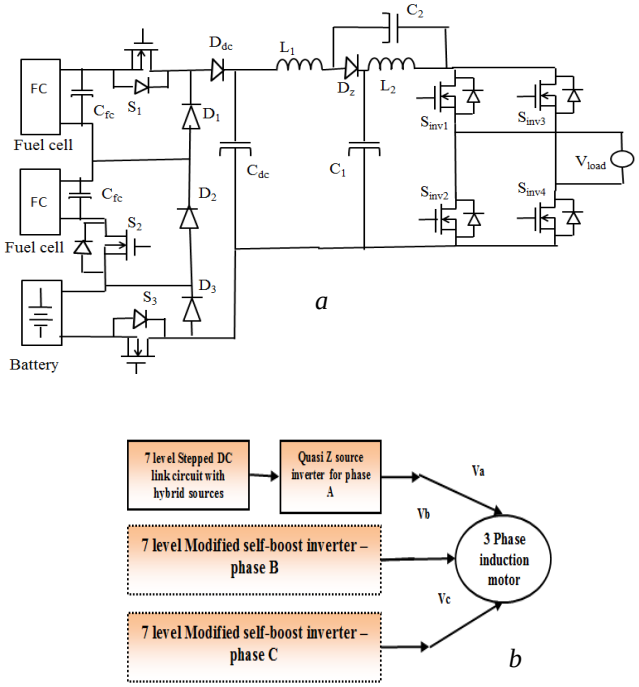

Fig. 3. Structure of (a) Proposed Single phase 7 level SDCqZSI (b) 3 phase 7 level SDCqZSI

Fig. 3b depicts the schematic of three phase SDCqZSI with a phase shift of 120 degree introduced in each phase. The output of the inverter is fed to three phase induction motor integrated with electric vehicle.

a. Switching Technique: Many switching strategies were devised for Z source inverters in literatures [18-22] of which maximum constant boost control with third harmonic injection is simple and provides high boost factor with constant shoot through and hence opted for the proposed inverter. Triangular carrier wave switched at high frequency is modulated with 180˚ phase shifted reference signals V_a and V_b and two constant lines V_p and V_n equal to magnitude of reference wave in positive and negative. The reference waveforms are defined by equation (1) and (2)

$$Va = 1.15MaSin(\omega_0 t) + 0.19MaSin(\omega_0 t) \quad (1)$$

$$Vb = 1.15MaSin(\omega_0 t - \pi) + 0.19MaSin(\omega_0 t - \pi) \quad (2)$$

Where Ma is the modulation index and ω_0 is the target output angular frequency.

Whenever the value of the reference signal and the constant line exceeds the carrier wave, firing pulse is generated.

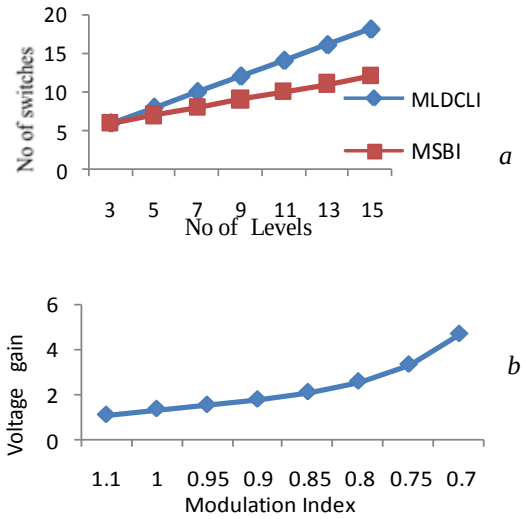

Fig. 4. (a)Switch requirement comparison and (b) voltage gain of SDCqZSI

A comparison is made between the switch count required for multilevel DC link inverter producing multilevel AC voltage without boost and the new topology of SDCqZSI inverter [23]. It is found from Fig. 4a. that the MLDCLI requires m+3 switches for m number of levels. The SDCqZSI requires only $\frac{[(m-1)]}{2}+4$ switches. This reduces the switch count considerably for higher levels. The voltage gain increases as Ma is decreased which is given in Fig. 4b.This is due to the increase in the duration of the shoot through states.

C. Operating Principle

The operating principle of the proposed inverter is simplified into two modes similar to its predecessor as shoot through mode and active mode, modelling equations are framed to arrive at the relation between the input and the output voltage.

a. Shoot through mode*:* This is the state when the legs of the inverter are short circuited, no power transmission happens and resulting in energy storage operation in impedance network. The power balance equation of the qZSI is given by (3)

$$V_b I_b (1 - D_s) = V_{ac} I_{ac} \qquad (3)$$

Where V_b represents the boosted stepped DC-link voltage, i_b is the current fed to the H bridge inverter, D_s is the shoot through duty ratio and V_{ac} and I_{ac} are the output voltage and current values. The equivalent circuit of the inverter during shoot through state is given in Fig. 5(d,e,f). Equal values of L and C were assumed for simplified analysis. The Vsdc is given by the equation (4).

$$V_{sdc} = V_1 + V_2 + V_3 + - - - + V_n \qquad (4)$$

KVL is employed to obtain the loop equations given by (5) and (5a)

$$V_{sdc} - V_{L1} + V_{c2} = 0 \qquad (5)$$

$$-V_{L2} + V_{C1} = 0 \qquad (5a)$$

Vsdc takes up the value of summation of FC and battery voltage depending on the switching.

b. Active mode*:* During the active state, the inverter is viewed as current source shown in fig. 5(a,b,c). The sum of input voltage and the energy stored in Z network appears at the output. The boosted multi-level DC link voltage V_b is given by (6)

V_b= V_{sdc}(=V_{in})+voltage in impedance network (6)

The generalised expression for V_b is given by (6a),

V_b= V_{sdc}(=nV_{in})+ voltage in impedance network (6a)

During the active state for a time period of T_{ns} the inverter operates as conventional voltage source inverter. The loop equations obtained by Kirchhoff's voltage law is given by (7)

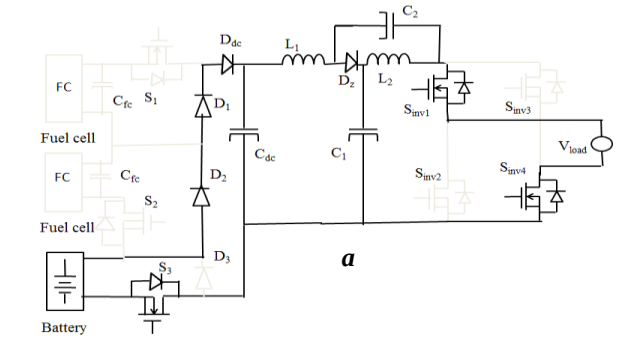

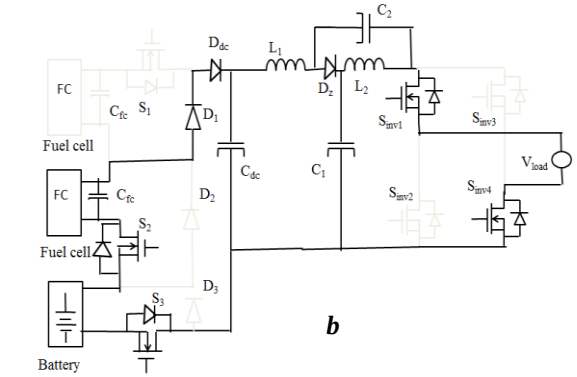

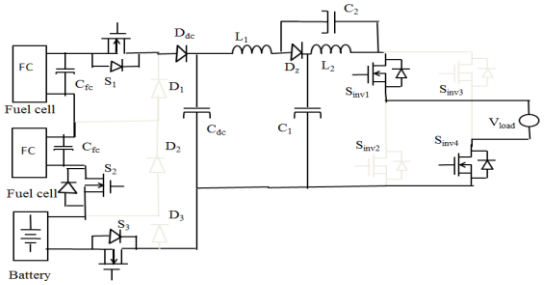

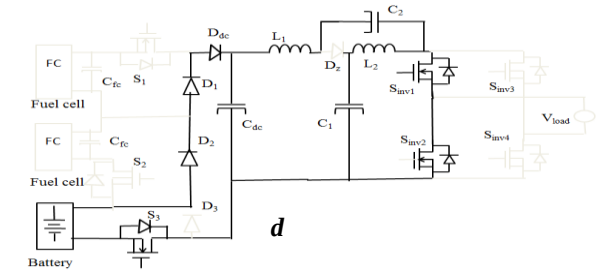

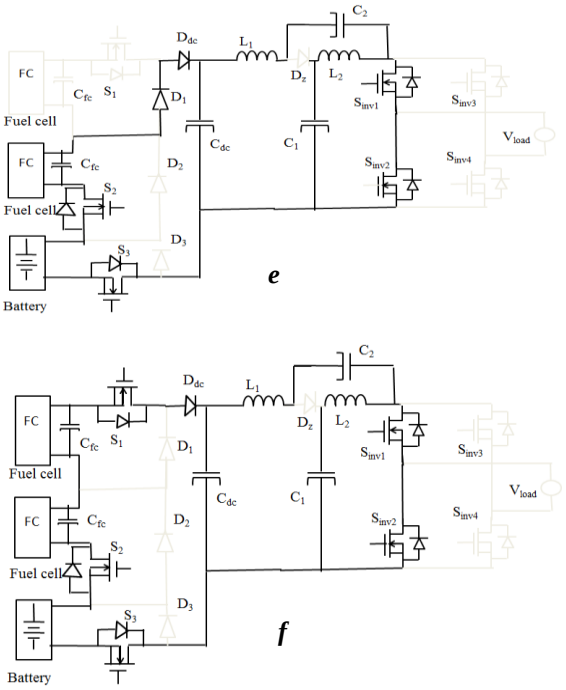

Fig. 5. Operation of SDCqZSI under shoot through mode and active mode

$$Vsdc - V_{L1} - V_{C1} = 0 \quad (7)$$

$$-V_{L2} - V_b + V_{C1} = 0 \quad (7a)$$

$$-V_{L2} - V_{C2} = 0 \quad (7b)$$

Modeling equations are derived to state the relation between input and output voltage in terms of the boost value. The voltage boost depends on the shoot through state which occupies a time period of T_s in the total switching time period of T_{tot}. The expression of total time period is given as $T_{tot} = T_s + T_{ns}$,

The average voltages of inductor 1 and 2 is equated to zero to get the expression for capacitor voltage through (8) to (11) from which the boost value of the inverter is arrived.

$$\frac{T_s(V_{sdc} + V_{c2}) + T_{ns}(V_{sdc} - V_{c1})}{T_{tot}} = 0 \quad (8)$$

$$\frac{T_s(V_{c1}) + T_{ns}(-V_{c2})}{T_{tot}} = 0 \quad (9)$$

$$Vsdc = \frac{-(T_s - T_{ns})}{T_{ns}} V_{c1} \quad (10)$$

Hence, $V_{c1} = \frac{T_{ns}}{T_{ns} - T_s} V_{sdc}$ and $V_{c2} = \frac{T_s}{T_{ns} - T_s} V_{sdc}$ (11)

On substitution and simplification of the above obtained equations in inductor voltage a relation between V_b and V_{sdc} is arrived which is depicted through (12) to (15),

$$V_{L2} = -V_b + \frac{T_{ns}}{T_{ns} - T_s} V_{sdc} \quad (12)$$

$$-\frac{T_s}{T_{ns} - T_s} V_{sdc} = -V_b + \frac{T_{ns}}{T_{ns} - T_s} V_{sdc} \quad (13)$$

$$V_b = \frac{T_{tot}}{T_{ns} - T_s} V_{sdc} \quad (14)$$

$V_b = B V_{sdc}$ and for n input sources, $V_{sdc} = n V_1$ (15)

The inverter output voltage is given by the expression (16)

$$V_{in} = M_a \frac{V_b}{2} \quad (16)$$

D. Power Loss Calculation

The power loss in qZSI includes loss in active state and shoot through state. The total loss comprises of loss in Z impedance network, switching loss and conduction loss.

a. Loss in Impedance network*:* The power loss in the capacitor and the inductor is accounted for loss in impedance network. The copper loss in inductor and capacitor is given by (17)

$$P_L = 2 I_L^2 R_L \text{ and } Pc1, c2 = 2 I_{c1}^2 R_c \quad (17)$$

where R_L and R_C are resistance of inductor and capacitor.

b. Switching loss*:* The switching loss includes the turn on/off of the MOSFET switches. The switching loss during the shoot through state is given by (18) and during the active state is given by (19) [24].

$$P_{sh} = (V_{sdc} I_{L1} \frac{T_{crt} + T_{vrt}}{2} + V_{sdc} I_{L1} \frac{T_{vrt} + T_{cft}}{2}) fs / 2 \quad (18)$$

$$P_{act} = Q_{rr} V_{sdc} fs + \frac{2}{\pi} \int_0^{\pi} ((V_{sdc} I_n \frac{T_{crt} + T_{vrt}}{2} + V_{sdc} I_n \frac{T_{vrt} + T_{cft}}{2}) \frac{fs}{2} d\omega t \quad (19)$$

Where Q_{rr} is the reverse recovery charge, I_{L1} is the current during shoot through and I_n is the current during active state.

E. Modeling of PEM Fuel Cell

Fuel cells have attracted interest in propulsion applications because of superior efficiency and zero emissions. Among many types of fuel cells, proton exchange membrane (PEM) fuel cell is being considered for automotive applications because of its low temperature operation and faster response [25-27].

Assuming constant temperature and oxygen concentration, the hydrogen PEM fuel cell can be modeled using the following mathematical equations from (20)-(23).The Voltage output of a single hydrogen fuel cell is expressed as (20)

$$V_{FC} = V_{NER} - V_{ACT} - V_{OHM} \quad (20)$$

The thermo dynamic potential of the cell stated as Nerst voltage is based on fuel concentration is given by (21)

$$V_{NER} = E_0 + \frac{RT}{2F} [\ln \frac{pH_2 pO_2^{1/2}}{pH_2O}] \quad (21)$$

Activation over-potential stated by (22) represents the voltage that is sacrificed to overcome the activation barrier to extract a net current from an electrochemical reaction.

$$V_{ACT} = \frac{RT}{\alpha F}\left[\ln\left(\frac{i}{i_0}\right)\right] \quad (22)$$

The ohmic over potential due to the electrical resistance of a fuel cell is given by (23)

$$V_{OHM} = i(R_m) \quad (23)$$

The mathematical model equations of the fuel cell presented is simulated and the characteristics are plotted. Fig. 6a,b shows the response of voltage and power of fuel cell for variation in current. The use of 37 cells produces an operating voltage of 60V for a current of 25A and the corresponding power is 1.5kW.

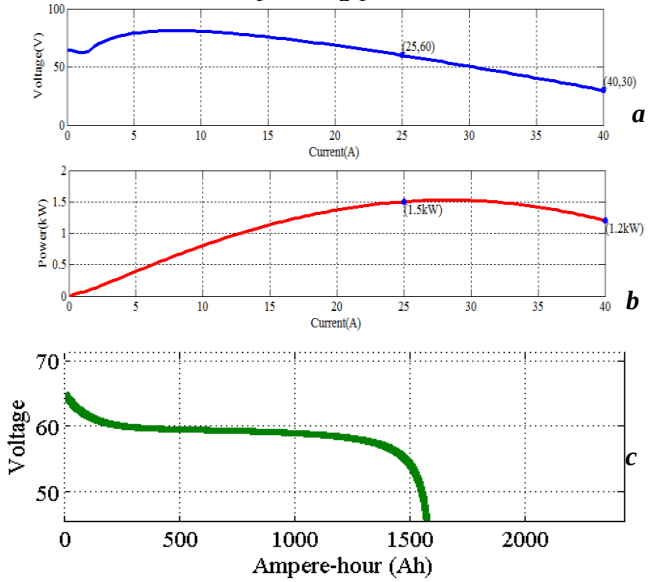

Fig. 6. Performance characteristics of fuel Cell and Battery

(a) , (b) Voltage and Power response of fuel cell for variation in current, (c) Voltage response of Battery

Battery is employed to handle load dynamics in HEV. It facilitates FC to operate in safe region during power demands. Fig. 6c.depicts the performance characteristics of battery with operating voltage of 60V.

4. Simulation and experimental results

A topology of seven level SDCqZSI was built in simulation corresponding to Fig. 3a with the parameters given in table 1.

Table 1
Simulation Parameters of SDCqZSI

Parameter	Value
Fuel cell voltage	60V
Battery voltage	60V
L_1=L_2	700µH
C_1=C_2	0.6µF
Stepped DC link frequency	50Hz
Inverter frequency	10kHz

A. *Performance analysis of Seven level SDCqZSI*

The performance characteristics of single phase seven level SDCqZSI with 0.87 power factor load is presented in Fig. 7a. A constant voltage of 60V fed from FC and battery produces a stepped DC link voltage of 180V. Operating the inverter at Ma=0.82 boosts the voltage to 320V and is flipped to produce seven level AC voltage. The load current approximates to a sinusoid of 6.2A. The capacitor voltage gradually increases to 240V and heavy stress is not witnessed. The input DC current does not show any noticeable inrush current during the starting.

The change in fuel cell voltage affects the inverter performance. The standard operating conditions are maintained by controlling the shoot through time period. A sudden withdrawal of a source reduces the stepped input voltage which is regained by controlling the modulation index as depicted in Fig.7b. The optimum Ma is identified for different input conditions to produce rated output voltage and is tabulated in Table 2. As the input voltage decreases, the Ma is decreased to increase the energy storage operation. This result in increased boost factor of the inverter, the stress on the device is also increased within appreciable limits.

Table 2
Optimum Ma for rated voltage at different input conditions (Vrms = 230V)

FC and Battery voltage (V)	Vsdc (V)	Ma for Vrated
70 each	210V	0.92
60each	180V	0.85
50each	150V	0.81
FC_1=40V, FC_2=60V , V_{bat} = 60V	160V	0.824
FC_1=60V,FC_2=30V, V_{bat}=20V	110V	0.76

Fig. 7a. depicts the modulation index for different voltage gain obtained by simple boost control and maximum constant boost control with third harmonic injection. The same voltage gain is obtained with higher modulation index in third harmonic injection and reduces the stress on the devices.

The effect of shoot through duty ratio for different input voltages is given in Fig. 7b. The increase in shoot through duty ratio has a direct impact on the boosted voltage and the component selection is greatly affected by this phenomena. The effect of shoot through duty ratios on capacitor voltages for different input voltage is shown in Fig. 7c. and Fig. 7d. As the boost value increases, an increase in stress is experienced and the capacitor 2 is prone to less stress compared to capacitor 1 in quasi Z network.

The steady state voltage at different stages of the proposed SDCqZSI is obtained to compare with conventional VSI, ZSI with input fed through a common DC bus and is tabulated in Table 3. It is very well seen that the SDCqZSI inverter perform buck

boost operation similar to its family and provides high boost value compared to ZSI. The VSI delivers reduced voltage on decrease of Ma and should be always operated with Ma=1 in association with DC-DC converter. It is seen that the stress on the capacitor in SDCqZSI is reduced compared to ZSI.

The voltage harmonic distortion is comparatively less and hence the filter requirement gets reduced. The THD increases on decrease of Ma due to the inclusion of more switching pulses.

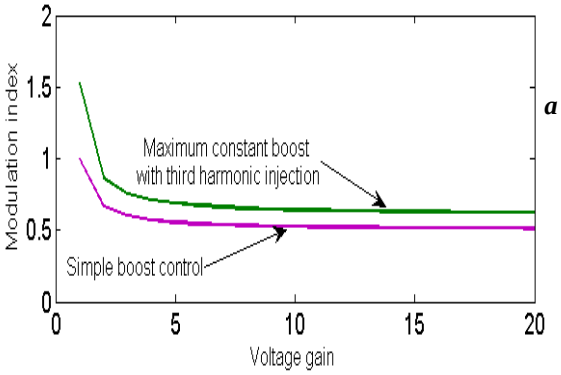

a

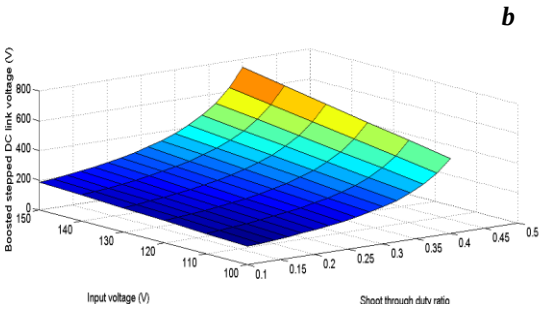

b

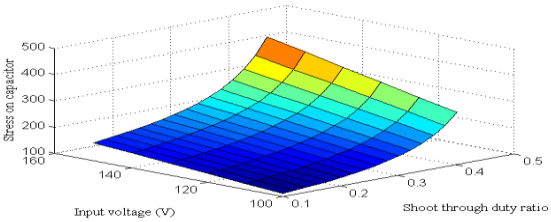

c

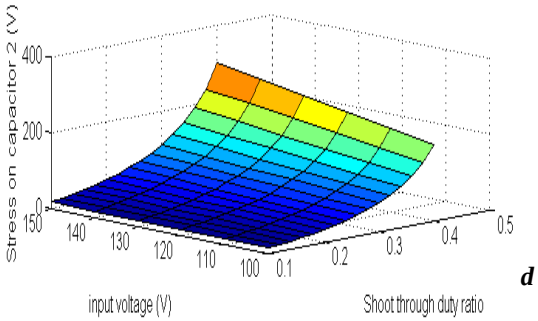

d

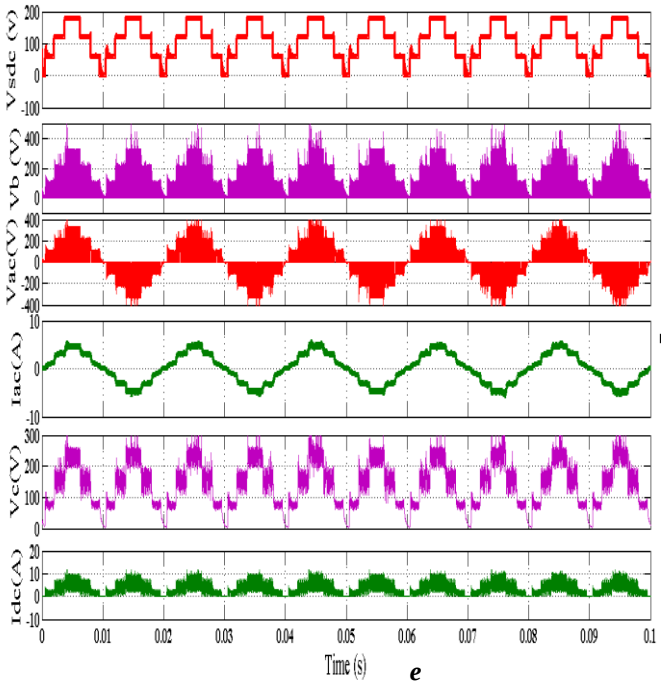

e

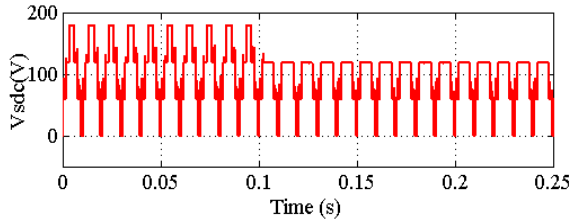

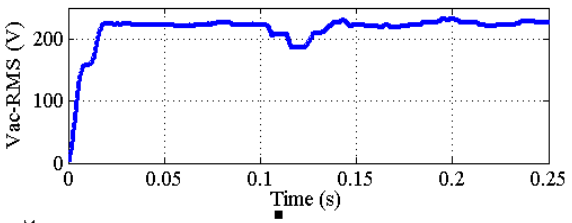

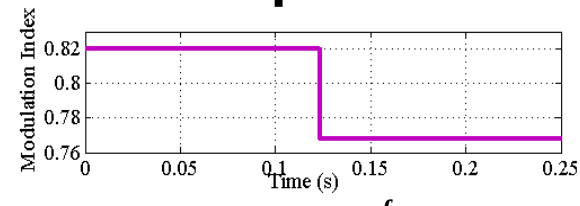

f

Fig . 7. Simulation response of SDCqZSI (a) Comparison of control techniques, (b)Effect of shoot through duty ratio on boosted DC link voltage, (c), (d) Effect of shoot through duty ratio on capacitor voltages, (e) Response at various stages of Inverter, (f) Control of output voltage by varying Ma

Table 3
Performance comparison of SDCqZSI, ZSI and VSI inverter for different Modulation indices

Ma	Vac(rms) V			Vb(V)			Capacitor voltage Vc (V)			THD		
	SDCqZSI	ZSI	VSI	SDCqZSI	ZSI	VSI	SDCqZSI	ZSI	VSI	SDCqZSI	ZSI	VSI
1	144	138	76.48	176	180		210	262		45.2	59.2	68.4
0.95	160	142	74.12	210	197		268	294		51.3	69.5	71.6
0.9	185	171	72.75	309	288	Not applicable	301	352	Not applicable	61.8	76.9	77.1
0.85	220	218	70.47	420	430		362	410		65.4	83	83.9
0.8	263	248	68.41	450	548		400	524		68.2	88.07	91.47
0.75	350	329	66.28	604	675		569	612		71.3	92.2	96.44

B.Performance Comparison of 3 phase Seven Level SDCqZSI with Motor Load

The three phase SDCqZSI inverter shown in Fig. 3. is integrated with induction motor to study the drive characteristics associated with HEV. The motor has to drive a load torque of 35N. A comparative evaluation of the SDCqZSI is made with the conventional VSI and ZSI integrated with traction motor and the parametric comparison is tabulated in Table 4. A 3 phase, 3.73kW, 415 V, 4 pole induction motor is used to study the simulation response.

It is very well seen that the source requirement is reduced and no inrush current is witnessed. The speed settles earlier and the ripple in torque is reduced by 4 Nm compared to VSI.

The voltage stress depends on the maximum working voltage the device is exposed. The DC link voltage and the capacitor voltage obtained in ZSI and SDCqZSI fed drive shown in the Fig. 8 reveals that the stress in the SDCqZSI fed drive is considerably minimized. The DC link voltage of ZSI fed drive has an overshoot of 1170V and settles at 820 V to obtain the rated voltage of 415V (line). The capacitor voltage peaks to 700V and settles at 570V. In case of SDCqZSI fed drive, the boosted voltage at DC link is 600V and the capacitor voltage is 480V. The stress is reduced by 16%.

Table 4

Performance Comparison of 3 phase Seven Level SDCqZSI with Motor Load

Parameter	VSI fed drive	ZSI fed drive	SDCqZSI fed drive
Source requirement	279FCs	155 FCs	111FCs
Input voltage	Constant DC	Constant DC	Stepped DC
Inrush current	1.7 times I_{final}	2times I_{final}	No inrush current
Settling time of speed	0.1 sec	0.06 sec	0.057 sec
Torque ripple	5 Nm	2 Nm	1 Nm

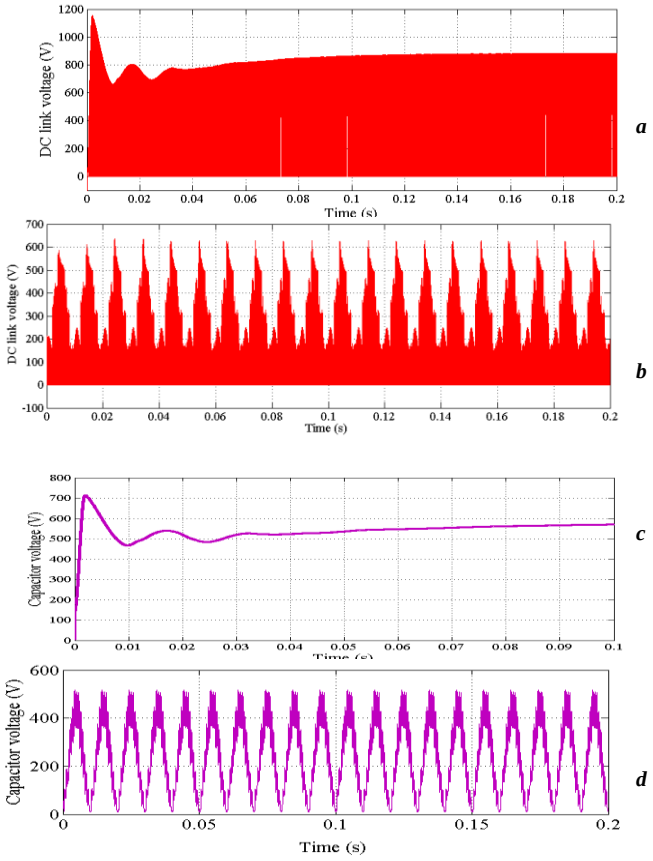

Fig. 8. DC link and Capacitor Voltage Comparison of SDCqZSI and ZSI fed drive at rated voltage (a), (c) ZSI fed drive (b), (d) SDCqZSI fed drive

Peak overshoot in voltage and heavy inrush of input current is not sensed (Fig. 9a, 9b) for motor load which is always a limitation in VSI and ZSI fed drive. This enhances reliable operation and reduces the component rating used in the system.

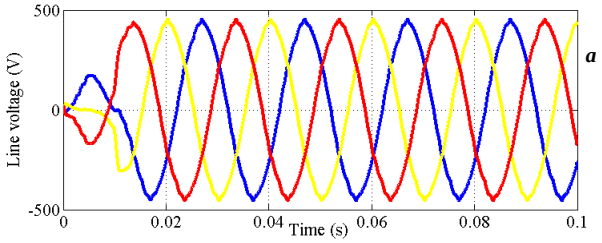

b

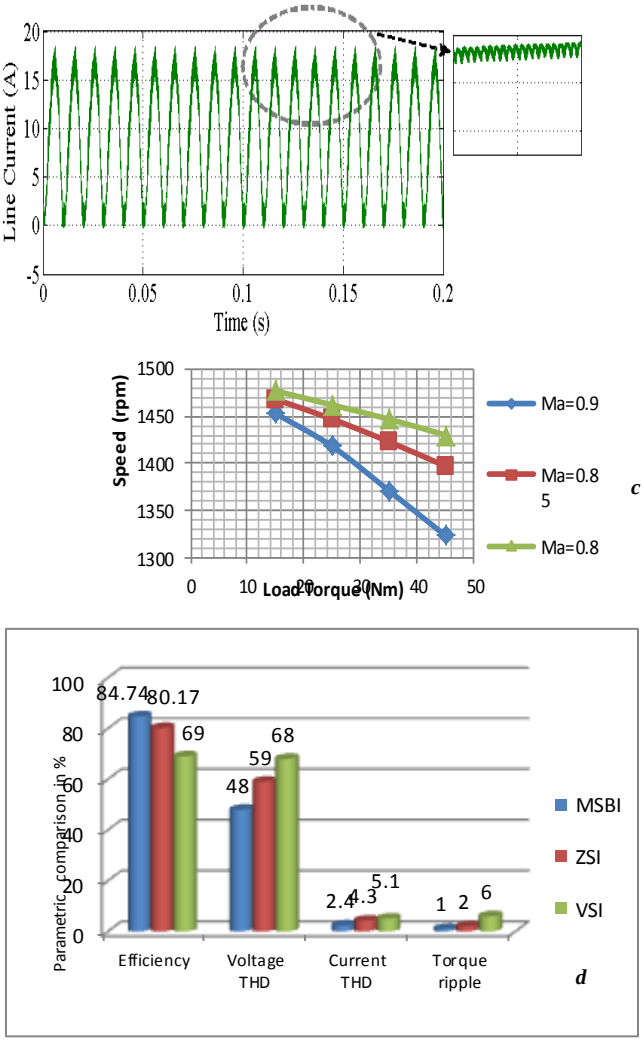

Fig. 9. Performance analysis of three phase SDCqZSIinverter (a)Line voltage(415V line) (b)DC Input current of SDCqZSI fed IM drive (18A)(c) SDCqZSI fed IM drive for different TL at various Ma(d) Performance comparison of SDCqZSI, ZSI and VSI fed IM drive of HEV

The acceleration and deceleration of the vehicle alters the load torque and the change in speed of the drive for various load torques at different modulation indices is shown in Fig.9c. The speed decreases with the increase in load torque. By altering the Ma, constant speed is maintained for different load torques. A comparative study is made on various parameters for the different inverter fed motor drive and is charted in Fig. 9d. The efficiency of the system is calculated by obtaining the power output and power input relations considering the switching losses and the loss encountered in the impedance network. The SDCqZSI fed IM drive shows a 4% improved efficiency compared to the ZSI fed drive system and 15% improved efficiency from VSI fed drive system. The voltage and current harmonic distortions are considerably mitigated and ripple in the torque is minimized in SDCqZSI.

A. Analysis of Hardware experimentation

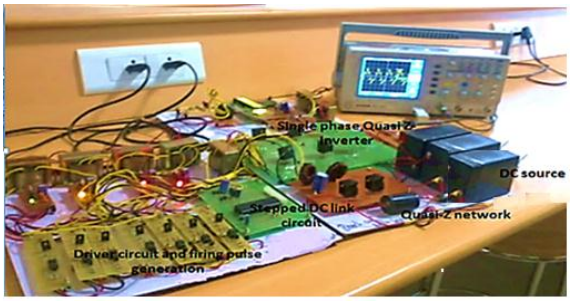

Fig.10.Experimental setup of single phase seven level SDCqZSI inverter

Tests on SDCqZSI were fulfilled in the experimental setup shown in the Fig. 10.The FC was replicated by 20V battery and three batteries are used as isolated energy source to synthesize 7 level output voltage. The circuit parameters of the inverter are

The stepped DC link voltage (V_{sdc}) for different input conditions having all the three sources, two sources and single source is shown in Fig. 11(d-f).

Fig. 11(g-i) shows the boosted multilevel AC voltage obtained from SDCqZSI. 60V is boosted to 108V with 7 levels in the output, 40V is boosted to 74V with 5 levels in the output and 38V with 2 level is obtained from 20V input for a Ma of 0.82. Continuous operation is ensured even during the failure of any source and the multilevel output mitigates the harmonics. The boosted voltage ranges from 108V to 38V which is very well within the voltage range of the capacitor and this shows that the device is subjected to reduced stress. The control over the modulation index delivers constant voltage to the load and stable operation is maintained.

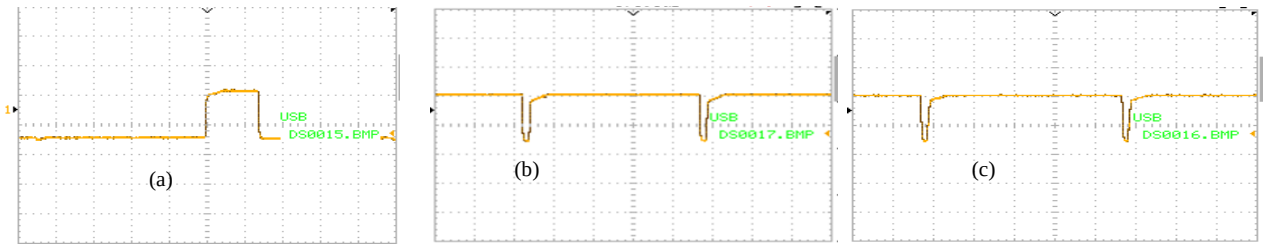

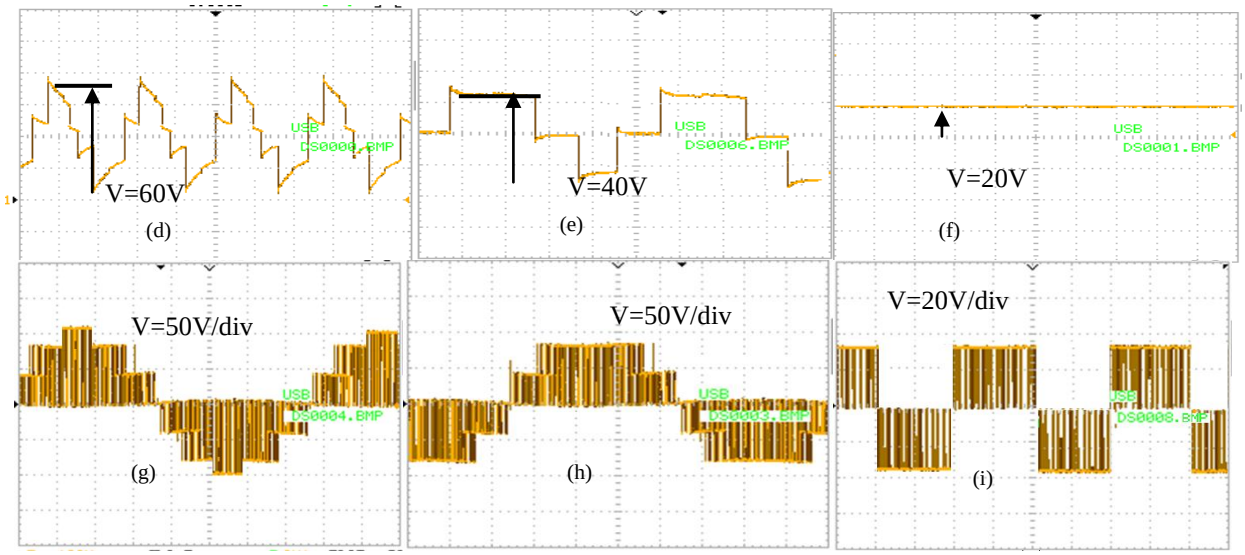

Fig . 11. Hardware output of gate pulse for stepped DC link circuit(a) S1, (b) S2, (c) S3, (d) Vsdc for three sources, (e) Vsdc for two sources, (f) Vsdc for single source, (g) Vac for Vsdc=60V, (g) Vac for Vsdc=40V, (g) Vac for Vsdc=20V at Ma=0.82

Table 5

Comparative study of Simulation and hardware results

Parameter	Simulation	Hardware
Boost factor	2	1.8
Vac (peak) for Vin=60V	117V	108V
Vc for Vin=60V	102V	89V
Efficiency	84.7	83.1

A comparative analysis between the simulation and hardware results is tabulated in Table 5. The hardware output matches the simulation performance and quantifies the advantage of the proposed inverter for HEVs.

5. Conclusion

This paper has presented an analytical model of stepped DC coupled qZSI for hybrid electric vehicles that links together the advantages of stepped DC link circuit with quasi Z source inverter. The proposed inverter minimizes the source requirements and offers optimum management with continuous operation of the drive. The performance comparison with different inverters comprehends that the SDCqZSI reduces the stress on the devices, the multilevel output minimizes voltage harmonics by 11% thus lowering the component rating and filter requirements. The absence of inrush current and high voltage during the start enhances safe operation of the inverter. The high boost factor enables only a small variation in modulation index that helps to control the stress within permissible limits. The analysis with induction motor drive demonstrated reduction in torque ripple by 1% with reduced settling time and improved efficiency of 4.5%. The steady state response of the prototype inverter in hardware well follows the simulation and the SDCqZSI enhances the performance of HEV.

APPENDIX

Nomenclature

V_{L1} ,V_{L2}	Voltage in inductors of impedance network
V_{sdc}	Stepped DC link voltage
V_{C1},V_{C2}	Voltage in capacitors of impedance network
V_b	Boosted DC link voltage
Ts	Time period of shoot through state
T_{ns}	Time period of active state
B	Boost value
Ma	Modulation index
n	Number of isolated energy sources
V_{FC}	Output Voltage of a single Fuel Cell in Volts
V_{NER}	Thermodynamic potential of the cell in Volts
V_{ACT}	Activation over potential in Volts
E_0	EMF of the cell at standard pressure
R, F	Universal gas constant in J/mol, Faraday's constant
P_{H2}, P_{O2}, P_{H2o}	Partial pressure of hydrogen, oxygen and water in atm
T	Temperature of the fuel cell
α	Charge transfer coefficient
i,i_0	Cell operating current, initial in Amps
R_m	Equivalent resistance of the fuel cell in ohms
T_{vrt}	voltage rise time during switching
T_{cft}	current fall time during switching
T_{crt}	Current rise time during switching
T_{vft}	voltage fall time during switching

REFERENCES

[1] Ehsani,Yimin Gao, Ali Emadi.: *Modern Electric, Hybrid Electric and Fuel cell vehicles, Fundamentals, theory and design*, CRC press, 2010.

[2] Schofield H.T., Yap, Bingham C. M.: *Hybrid energy sources for electric vehicle and fuel cell vehicle propulsion*, IEEE Transactions on Vehicular Technology 2005, Vol. 21, p. 42-50.

[3] Bayindir K.C., Gozukucuk M.A., Teke A.: *A comprehensive overview of hybrid electric vehicle: Powertrain configurations, powertrain control techniques and electronic control units*,Energy Conversion and Management, Elsevier 2011, Vol. 52,p. 1305- 1316.

[4] Ali Emadi, Sheldon S., Williamson, Alireza Khaligh: *Power electronics intensive solutions for advanced electric, hybrid electric, and fuel cell vehicular power systems*, IEEE Transactions on Power Electronics 2006, Vol. 21, p. 567-576.

[5] Young-Joo Lee, Khaligh A., Emadi: *Advanced Integrated Bidirectional AC/DC and DC/DC Converter for Plug-In Hybrid Electric Vehicles*, IEEE Transactions on Vehicular Technology 2009, Vol. 58, p. 3970- 3978.

[6] Umamaheswari S., Thakura P.R., Keshri R.K.: *Hardware development of Voltage Source Inverter for Hybrid Electric Vehicle*, Int Proceedings on Electrical Energy Systems (ICEES), Newport Beach, CA, 67, 2011

[7] Peng F. Z.: *Z-source inverter*, IEEE Transactions on Industrial Applications 2003, vol. 39, no. 2, p. 504–510.

[8] Liqiang Yang, Dong yuan Qiu, Bo Zhang, Guidong Zhang, *High-performance quasi-Z-source inverter with low capacitor voltage stress and small inductance*, IET Power Electronics 2015, Vol. 8, p. 1061-1069.

[9] Meenakshi T., Suthanthira Vanitha N., Rajambal K.: *Investigations on Solar Water Pumping System with Extended Self Boost Quasi Impedance-Source Inverter*, 2013 IEEE Int. Conf. ICEETS 2013, Nagerkoil.

[10] Yu Tang, ShaojunXie, Chaohua Zhang, and Zegang Xu: *Improved Z-Source Inverter With Reduced Z-Source Capacitor Voltage Stress and Soft-Start Capability*, IEEE Transactions on Power Electronics 2009, vol. 24, no. 2,p. 409-415.

[11] Gajanayake, C. J., Fang Lin Luo, Hoay Beng Gooi, et. al.: *Extended boost Z-source inverters*, IEEE Transactions on Power Electronics 2010, vol. 25, no. 10, p. 2642-2652.

[12] Sun D., Ge. B., Yan X., Zhang H., Liu Y., Abu Rub H., Ben Brahim L., Peng FZ.: *Modeling, Impedance design and Efficiency Analysis of Quasi –Z source Module in Cascaded Multilevel Photovoltaic power system*, IEEE Transactions on Power Electronics 2014, Vol. 61, p. 6108-6117.

[13] Peng FZ., Shen M., Holland K.: *Application of Z-source inverter for traction drive of fuel cell-battery hybrid electric vehicles*, IEEE Transactions on Power Electronics 2007, vol. 22, no. 3, p. 1054–1061.

[14] Dehghan S. M, Mohamadian M., Yazdian A.: *Hybrid electric vehicle based on Bi-directional Z-source nine-switch inverter*, IEEE Transactions on Vehicular Technology 2010,Vol. 59, p. 2641-2643.

[15] Ellabban O., Van Mierlo J., Lataire P., Van Den Bossche P.: *Z -source inverter for vehicular applications*, Proceedings Int. Conf. IEEE Vehicle Power and Propulsion Conference, pp. 1,2011.

[16] Omar Ellabban, Joeri Van Mierlo, Philippe Lataire: *Control of a Bidirectional Z-Source Inverter for Electric Vehicle Applications in Different Operation Modes*, Journal of Power Electronics 2011, Vol. 11, p. 120-129.

[17] Dorrell D. G., Popescu M., Evans L., Staton D. A., Knight A. M.: *Comparison of Permanent Magnet Drive Motor with a Cage Induction Motor Design for a Hybrid Electric Vehicle*, Proceedings. Int. Conf. Power Electronics, Sapporo, Japan, June, pp. 21-27, 2010.

[18] Tang Y., Xie S., Ding J.: *Pulse width modulation of Z-source inverters with minimum inductor current ripple*, IEEE Transactions on Industrial Electronics 2014, Vol. 61, p. 98-106.

[19] SonyBabu C.M., Meenakshi T., Suthanthira Vanitha N.: *Space Vector PWM for Quasi-Z Source Inverter with Battery based PV Power Generation System*, 2015 Int. Conference proceedings. *ICCCT 2015*.

[20] BahramRashidi: *FPGA Implementation of Digital Controller for Simple and Maximum Boost Control of Three Phase Z-Source Inverter*, I.J. Information Technology and Computer Science 2013, Vol. 04, p. 85- 94.

[21] Shen M., Wang J., Joseph A., Peng F. Z., et. Al: *Constant Boost control of the Z-source inverter to minimize current ripple and voltage stress*, IEEE Transactions on Industrial Applications 2006, vol. 42, no. 3, p. 770–777.

[22] Liu Y., Ge B., Abu-Rub H., Peng F.Z.: *Phase-shifted pulse-width-amplitude modulation for quasi-Z-source cascade multilevel inverter-based photovoltaic power system*, IET Power Electronics 2014, Vol. 7, p. 1444-1454.

[23] Gui-Jia Su: *Multilevel DC-Link Inverter*, IEEE Transactions On Industrial Applications 2005,Vol. 41, p. 848-856.

[24] Graovac D., Purschel M., Kiep A.: *MOSFET power losses calculation using the data-sheet parameters*, Automotive Power *2006*, Application Note, 1.1.

[25] Gao F., Blunier B., Simoes M., Miraoui A.: *PEM fuel cell stack modeling for real-time emulation in hardware-in-the-loop applications*, IEEE Transactions on Energy Conversion 2011, Vol. 26, p.1-9.

[26] Powell B.K., Bailey K.E., Cikanek S.R.: *Dynamic Modeling and Control of Hybrid Electric Vehicle Powertrain Systems*, IEEE Transaction on Control System 1998, p.17-33.

[27] Jeferson Marian Correa, Felix Alberto Farret, Luciana Neves Canha: *An analysis of the dynamic performance of proton exchange membrane fuel cell using an electrochemical model*, IEEE Transaction on Industrial Electronics 2001, p 141-146.

[28] Bharatiraja1 C., Latha: *A New Asymmetrical Single Phase 15 Level Reduced Switch Multilevel Voltage Source Inverter*, Journal of Electrical Engineering 2015, Vol. 15, p.1-9.